Journal of Engineering Science and Technology
Vol. 12, No. 9 (2017) 2374 - 2392

GREY RELATIONAL ANALYSIS AND ITS APPLICATION ON SURFACE PROPERTIES DURING EDM AND POWDER MIXED EDM

S. TRIPATHY*, D. K.TRIPATHY

Mechanical Engineering Department, Siksha 'O' Anusandhan University,
Bhubaneswar-751030, India
Indian Institute of Technology, Kharagpur, India
*Corresponding Author: sasmeetatripathy@soauniversity.ac.in

Abstract

Electrical discharge machining is an extensively used non-conventional process for material removal in die manufacturing and aerospace industries. The mechanism of powder mixed electric discharge machining is very different from that of electrical discharge machining process. It was found that considerable research has been done on different aspects during electric discharge machining of various steels, but sufficient data is not available on the surface properties and optimum process parameters for machining of H-11 die steel. The present work investigates the effect of process parameters like powder concentration, peak current, pulse-on-time, duty cycle and gap voltage on material removal rate, surface roughness, recast layer thickness and micro-hardness simultaneously during electrical discharge machining and powder mixed electrical discharge machining of H-11 hot work tool steel. Multi-objective optimization using grey relational analysis was used to determine the optimal setting of process parameters for maximum material removal rate, minimum surface roughness, minimum recast layer thickness and maximum micro-hardness simultaneously. The work material has been selected due to its brilliant mechanical properties and diverse industrial applications. Taguchi's L_{27} orthogonal array was used to carry out the experiments. Analysis of variance was performed to determine the significant parameters at a 95% confidence interval. Conductive powder mixed to the dielectric fluid was graphite of size less than 53µm obtained from the sieve analysis. Electrolytic copper was used as the tool electrode. Investigation of micro-structures was done using scanning electron microscope to examine alterations and defects on the machined surface. Grey relational analysis exhibits an improvement of 0.2025 in the grey relational grade. The tendency of deviation of the response curves suggest that powder concentration of 0g/l, peak current of 3A, pulse-on-time of 150µs, duty cycle of 70% and gap voltage of 30V offer maximum grey

Nomenclatures

C_p	Concentration of graphite powder, g/l
DC	Duty Cycle
HVN	Micro-hardness
I_p	Input Current, A
MRR	Material Removal Rate, mm^3/min
RLT	Recast layer thickness, µm
SR	Surface Roughness R_a, µm
T_{on}	Pulse on time, µs
V_g	Gap voltage, V

Abbreviations

ANOVA	Analysis of variance
EDM	Electrical discharge machining
GRA	Grey Relational Analysis
GRC	Grey Relational Coefficient
GRG	Grey Relational Grade
PMEDM	Powder mixed electrical discharge machining

relational grade when machined during electrical discharge machining and graphite powder mixed electrical discharge machining. The surface properties during powder mixed electrical discharge machining using graphite powder do not show much improvement in comparison to machining without addition of powder due to the significant formation of carbide layer on the top surface of the machined specimen which increase the micro-hardness thus leading to crack formation and propagation.

Keywords: EDM, PMEDM, Multi-objective optimization, Grey relational analysis, Material removal rate, Surface roughness, Recast layer thickness, Micro-hardness, SEM.

1. Introduction

Electrical discharge machining (EDM) process is being widely used throughout the globe to impart intricate shapes to conductive metals and alloys possessing high hardness, toughness and finding huge application in the mould and die making industries, aerospace, automobile and electronic industries. Powder mixed electrical discharge machining (PMEDM) has developed out of the requirement to conquer these margins and develop the machining potential of EDM. PMEDM involves the adding up of a proper material in a fine powdered form to the dielectric fluid which in turn decreases the insulating strength of the dielectric fluid and increases the inter-electrode gap causing an easy removal of debris.

Material removal occurs under suitable conditions, wherein, the removed material combined with the powdered particles deposit on the workpiece surface modifying and improving the surface properties. As the sparking pattern changes due to the presence of abrasive powders, there is a lot of alteration in the machined surface properties.

The past research in EDM deals with a lot of development in the direction of controlling and optimizing the process parameters, predicting and improving the process characteristics with increased material removal rate (*MRR*), low tool wear rate (TWR), low surface roughness and improved surface properties. Alloying elements can be added from the electrode to the machined surface during the end of the machining or some suitable fine powder can be added to the dielectric for the modification of the surface properties by material transfer and deposition mechanism which thus increases the hardness of the machined surface and improves the surface quality [1-3]. Pecas and Henriques [4, 5] suggested that PMEDM is an emerging technique which has given a new direction to improve the process capabilities and produce near mirror like surface finish with reduced surface cracks and homogenization of the white layer. The investigation on the performance of the PMEDM process depends upon characteristics like powder type, concentration, particle size, electrode area, work-piece constituents and properties. Kumar et al. [6] reported reviews on the effect of mixing different powders and additives to the dielectric. Kumar et al. [7] observed the material transfer from Cu, Cu-Cr and Cu-W electrodes to AISI H13 die steel in presence of tungsten powder suspended in the dielectric. Jeswani [8] concluded that suspension of powdered graphite to kerosene improved the rate of material removal by 60% and decreased the TWR by 15%.

Kansal et al. [9, 10] studied the effect of process parameters to determine the optimal setting of parameters for PMEDM using response surface methodology, Taguchi, utility concept and multi-objective optimization. Singh and Yeh [11] used grey relational analysis to optimize multiple responses while machining aluminium matrix composites using SiC powder to obtain the optimum parameters for machining. Bhattacharya et al. [12] identified the suitable parameter set for rough and finish machining on EN-31, H-11 and HCHCr die steel using aluminium and graphite powders with different combinations of tool and dielectric. Singh et al. [13] evaluated the role of input parameters on surface roughness while machining H-11 die steel using copper tool and by adding Al powder to the dielectric. The surface roughness was improved and negative polarity of the tool electrode was found desirable for lowering the surface roughness. Effect of the addition of silicon and aluminium powder to the dielectric on the process parameters has also been investigated [14-16]. Silicon powder having particle size of 10-30µm when machined at low current produced fine and corrosion resistant surfaces of roughness less than 2µm [17-19].

The past studies depict that different studies have been made in the field of EDM and PMEDM and results have been reported by adding different powders mixed to the dielectric fluid, but not much work has been done on the performance characteristics of the PMEDM process on H-11 die-steel. PMEDM involves a large number of input process parameters that control the quality of the machined component. Therefore, the relative significance of the process variables on output responses is worth investigating. The surface characteristics and micro-hardness during the machining of H-11 using graphite powder mixed EDM in varying concentrations has not been investigated thoroughly and it is still under experimentation. Comparative studies between EDM and PMEDM using graphite powder on H-11 work material has not been much investigated. The recast layer formation with difference in concentration of powder on H-11

die steel needs to be investigated experimentally. The alterations occurring in the surface characteristics due to the addition of powder have to be understood in depth. Multi-attribute decision making techniques have not been much implemented to find the optimal setting during PMEDM of H-11. Thus, the analysis of improvement occurring in the process using multi-attribute optimization techniques is desirable to increase the efficiency of the process and the achieved surface quality. The present work is a step in this direction. An attempt has been made to find out the best possible set of process variables through multi-objective optimization using GRA to acquire maximum *MRR*, minimum surface roughness R_a (SR), minimum recast layer thickness *(RLT)* and maximum micro-hardness (*HVN*) using graphite powder mixed to the dielectric fluid. Analysis of variance *(*ANOVA*)* was used to locate the statistically significant input parameters affecting the output responses.

2. Experimental Details

Experiments were performed on die sinking type EDM (model Electronica Smart ZNC) with positive polarity and servo-head. Commercial grade EDM oil was used as dielectric fluid. For minimization of the cost and effective use of dielectric fluid and powder particles, a detachable tank was designed as shown in Fig. 1. The newly designed and modified tank was placed in the main machining tank and was isolated from the filtering system of the machine. This newly designed tank was used as the working tank for the entire machining process. To ensure proper distribution of powder in dielectric fluid throughout the machining cycle, a pump and stirring arrangement was installed to the working tank. Required amount of powder was suspended to the dielectric fluid uniformly with constant stirring action to avoid the non-uniformity in the mixture and settling down of the powder at the bottom of the tank. The amount of powder to be suspended was measured with the help of an accurate weighing balance. With the change in concentration of powder after nine runs, a freshly prepared mixture of dielectric fluid and powder particles with desired concentration was added to the tank for machining thus maintaining the powder concentration thoroughly throughout the machining cycle. Each run was carried out for time duration of 15minutes. Workpiece material selected for the experiment was H-11 die steel which is a hot work steel possessing very high hardenability, toughness, high abrasion resistance, excellent wear resistance and high compressive strength.The typical applications of this grade of steel is found in a wide range of aircraft and structural use, die casting dies, piercing tools, extrusion tooling, forging dies, punches. The chemical composition of the workpiece is given in Table 1. The dimension of the workpiece is 120×60×25 mm obtained in proper annealed condition. The tool electrode selected for the experiment is electrolytic copper having a dimension of 20×20×60 mm.

3.Design of Experiments

3.1. Selection of factors and their levels

Taguchi's Technique was implemented to find the effect of process variables on the PMEDM performance. The important input parameters selected were concentration

of graphite powder (g/l), I_p, T_{on}, *DC* and V_g varying at three levels respectively based on certain pilot experiments performed for selection of parameters and their levels as shown in Table 2. The influence of input parameters on response variables like *MRR, SR, RLT and HVN* was examined. Considering the number of factors and their levels an L_{27} Taguchi's orthogonal array was used to perform the experiments.

Table 1. Original chemical composition of the workpiece.

Element	Composition (wt.%)
Carbon	**0.39**
Silicon	**1**
Manganese	**0.5**
Phosphorous	**0.03**
Sulphur	**0.02**
Chromium	**4.75**
Molybdenum	**1.1**
Cobalt	**0.01**
Copper	**0.01**
Vanadium	**0.5**
Iron	**Balance**

Fig. 1. Experimental setup.

Table 2. Selection of levels for the factors.

Factors with units	Levels		
	Level 1	**Level 2**	**Level 3**
Concentration of graphite powder (g/l)	0	3	6
Peak Current (A)	3	6	9
Pulse On Time (µs)	100	150	200
Duty Cycle (%)	7	8	9
Gap Voltage (V)	30	40	50

3.2. Taguchi technique:

Taguchi's process uses means to normalize the functions. Signal to noise (S/N) ratio is considered to minimize the variations in the output responses obtained from the experimental data. S/N ratio is defined as the ratio of mean of the signal to the standard deviation of the noise. It is denoted by 'η' with a unit of dB. Depending upon the type of characteristics, S/N ratio is of three types like higher the better (HB), Lower the better (LB) and nominal the best (NB). The following equations are used to calculate the S/N ratio in the present study:

$$\text{HB: S/N Ratio} = -10\log_{10}\left[\frac{1}{n}\sum_{i=1}^{n} y_i^{-2}\right] \tag{1}$$

$$\text{LB: S/N Ratio} = -10\log_{10}\left[\frac{1}{n}\sum_{i=1}^{n} y_i^{2}\right] \tag{2}$$

where y is the sample mean for the number of observations in each trial.

3.3. Multi-objective optimization using grey relational analysis:

In GRA, the experimental values of the measured quality feature are normalized within a range of zero to one. This can be identified as grey relational generation. The grey relational coefficient (*GRC*) is then computed. Overall performance characteristic depends on the computation of the grey relational grade (GRG). Thus, a multi-attribute process optimization is transformed to a single objective problem. The highest GRG will be evaluated as the optimal parametric combination. For grey relational generation, the *MRR* and *HVN* consequent to higher the better principle is given as:

$$x_i(q) = \frac{y_i(q) - \min y_i(q)}{\max y_i(q) - \min y_i(q)} \tag{3}$$

SR and RLT subsequent to lower the better condition are specified as:

$$x_i(q) = \frac{\max y_i(q) - y_i(q)}{\max y_i(q) - \min y_i(q)} \tag{4}$$

where $x_i(q)$ is the value obtained for grey relational generation, min $y_i(q)$ is the least value of $y_i(q)$ for the q^{th} response and max $y_i(q)$ is the largest value for the q^{th} response, where q = 1, 2, 3, 4 for the various output responses considered in a sequence. The data after normalization for the 'grey relational generation' is calculated. The *GRC* is computed to establish a correlation between the finest data and the definite normalized data. The *GRC* is calculated as:

$$\xi_i(q) = \frac{\Delta_{\min} + \psi\Delta_{\max}}{\Delta_{0i}(q) + \psi\Delta_{\max}} \tag{5}$$

where $\Delta_{oi}(q) = \left| x_o(q) - x_i(q) \right|$, ψ is the distinctive coefficient lying between $0 \leq \psi \leq 1$, Δ_{min} is the minimum value for Δ_{oi} and Δ_{max} is the maximum value for Δ_{oi}. The GRG can now be formulated as:

$$\gamma_i = \frac{1}{n}\sum_{q=1}^{n} \xi_i(q) \tag{6}$$

where n is the number of output responses. The high is the value of GRG, the subsequent arrangement of parameters is closer to the optimum solution.

4. Results and Discussion

4.1. Effect of input parameters on material removal rate

The machining efficiency of the process can be characterised by the material removal rate of the workpiece. The main aim behind machining should be more amount of material removal with less tool wear. Figure 2(a) shows that with the increase in current, the MRR tends to increase. This is because with the increase in electrical power, additional thermal energy is generated in the discharge channel. Addition of powder particles to the dielectric fluid causes decrease in insulating strength of the dielectric fluid and the inter-electrode gap increases causing an easy removal of debris. Due to the bridging effect, quicker sparking occurs resulting in faster erosion from the workpiece surface. This easy short circuit improves the machining rate of the process. The plasma channel gets widened and enlarged, producing stable and uniform sparks. Thus thin craters are formed on the workpiece which improves the surface quality. Figure 2(b) shows that when C_p is 3 gm/l, the MRR increases and as the C_p increases to 6 gm/l, the MRR further increases with the increase in I_p. Figure 2(c) shows that the MRR increases with the increase in T_{on} as more heat is transferred to the section which consequently removes more amount of material from the workpiece surface thus improving the machining rate. Figure 2(d) exhibits that as the duty cycle increases, the MRR initially shows very minimal rise but gradually it increases tremendously with further increase of duty cycle as the ejection of molten material occurs rapidly. Increase in gap voltage increases the discharge gap distance increasing the deposition of material on the machined surface, hence, if proper flushing is maintained, then the MRR increases with the increase in the gap voltage which is demonstrated in Fig. 2(e).

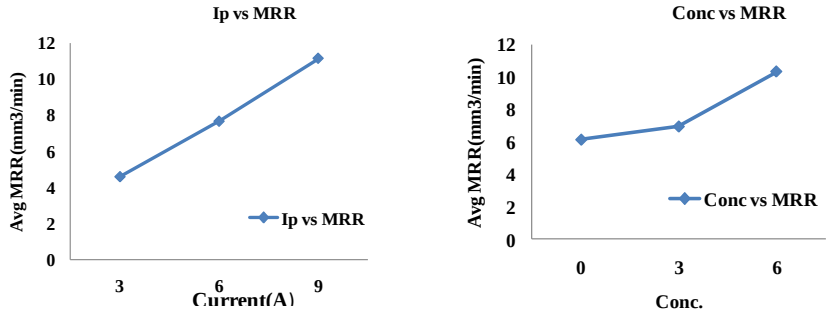

(a) **(b)**

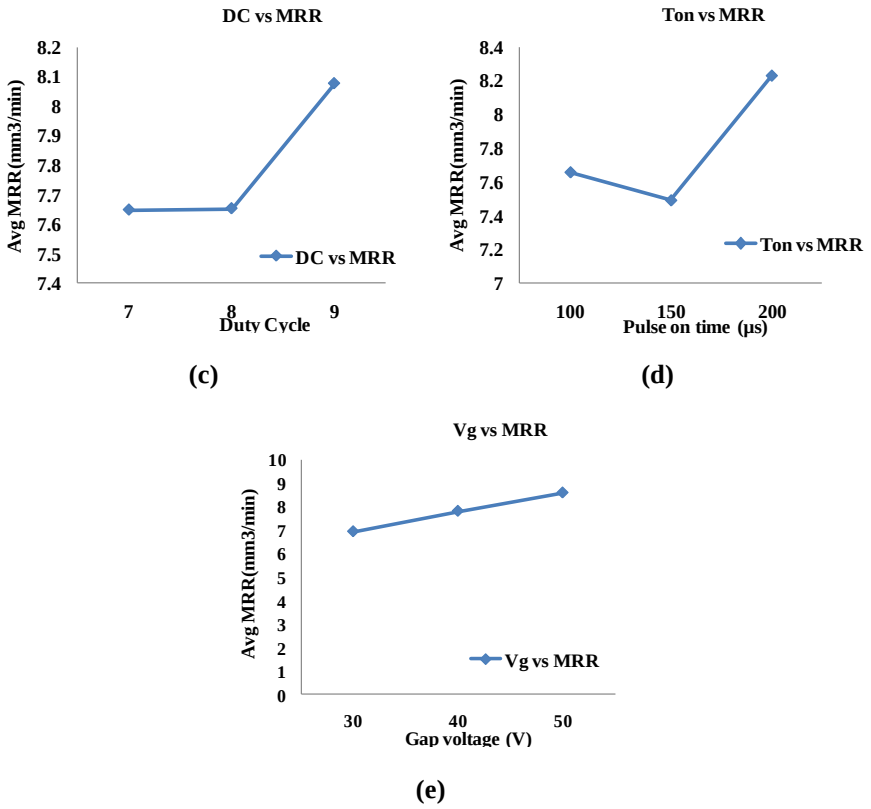

Fig. 2.Variation of material removal rate (MRR) with input parameters.

4.2. Effect of input parameters on surface roughness

The roughness of an electro-discharge machined surface is correlated to the size of the crater formed and the variation of recast layer on the surface formed because of melting and evaporation. When the cooling takes place during flushing, some amount of molten material solidifies on the surface increasing the roughness. During PMEDM, the surface texture improves due to reduced roughness. The surface roughness has been considered as the arithmetic mean of roughness obtained for the examined surface using a surface roughness tester. Figure 3(a) shows that the increase in pulse current increases the roughness of the surface because the huge dispersive energy causes aggressive sparks and impulsive forces resulting in creation of larger craters thus increased surface roughness. Figure 3(b) shows that the powder concentration plays an important role as the roughness values are reduced with the increase in concentration of powder. The *SR* is maximum during EDM, when no powder is added to the dielectric fluid. The *SR* remarkably reduces during PMEDM when the powder is added in the concentration of 3g/l. Adding powder in a concentration of 6g/l to the dielectric fluid, slightly increases the *SR*. Addition of powder particles in proper concentration reduces the *SR* during machining. Addition of more amount of powder will cause difficulty in stirring as it settles down in the tank and affects the surface properties of the material. On adding powder particles, the bridging

effect takes place beneath the sparking area causing multiple discharges on one pulse which thus creates faster sparking and erosion from the workpiece surface. This easy short circuit improves the machining rate of the process. The plasma channel gets widened and enlarged, producing stable and uniform sparks forming shallow craters on the workpiece surface with enhanced surface quality and reduced *SR*. Figure 3(c) shows that as the pulse on time is increasing, the SR also increases. This may be due to more amount of heat being transferred to the section. As the flushing pressure remains constant, the dielectric fluid cannot flush the molten material and debri particles thus increasing the roughness of the surface. Figure 3(d) shows that with the increase in the duty cycle the SR initially decreases and then subsequently increases.

During PMEDM, the plasma flushing efficiency increases which causes ejection of molten metal consequently decreasing the re-solidification of thus improving the surface texture. Further increasing the concentration of powder, subsequently increases the roughness of the surface due to deposition and formation of carbide layers on the top surfaces. The increase in V_g increases the SR as represented in Fig. 3(e) due to the fact that increasing the gap voltage increases the discharge gap distance which reduces the effect of induced energy at the workpiece and increases the deposition on the machined surface thus increasing the SR. The surface roughness measured from micro-topography (S_a) was also measured as the actual deviation from the nominal surface by considering the micro-structural analysis. The variation of the material surface beneath the recast layer can be seen from the micro-structural studies shown in Fig. 4. It can be explained that the roughness of the surface is dependent on the recast layer distribution. The material beneath the recast layer and heat affected zone also gets affected due to the evaporation, melting and re-solidification of the molten material and the prevailing temperature conditions. It may also be observed from Fig.4, that the inclined red lines represent the position of the crack formation at different location in the sampling length and the vertical red line shows the maximum thickness of the recast layer. The cracks formed near the crest region are more intense due to the stress accumulation and also the cracks propagate and penetrate to the base material. The cracks formed near the trough region are less intense as compared to the cracks in the crest.

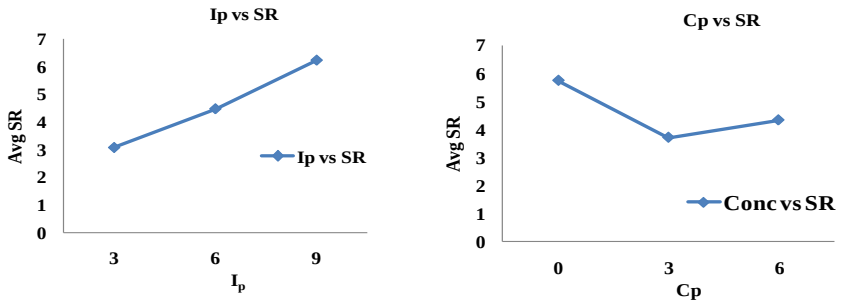

(a) **(b)**

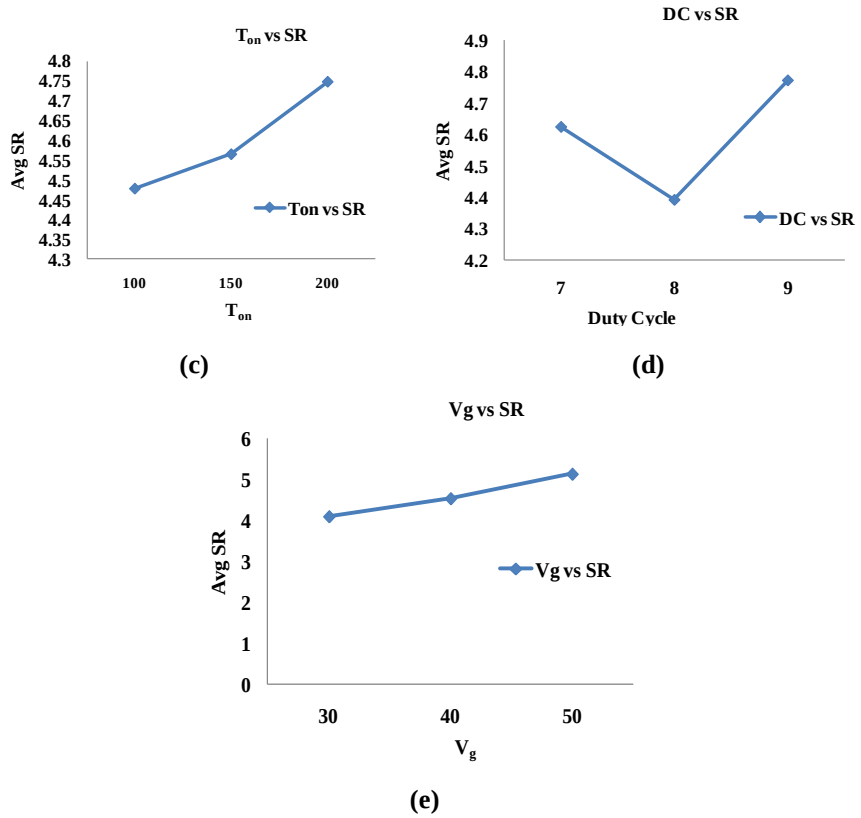

Fig. 3. Variation of surface roughness *Ra* (SR) with the input parameters.

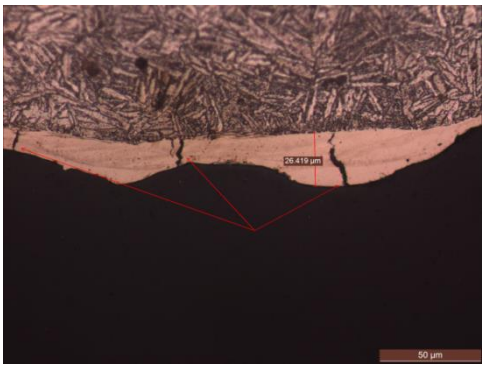

Fig. 4. Micro-structure representing **surface roughness R_a (SR) and *RLT*.**

4.3. Effect of input parameters on recast layer thickness

The faster machining rates produce higher *RLT*. Reducing the recast layer formation and improving material properties are the goal in the field of EDM. It can be seen from Figure 5(a) that the *RLT* value rises with the rise in I_p as the

surface temperature reaches the melting temperature leading to greater material removal. The dielectric fluid is unable to remove the molten material in the specified time duration thus enhancing the *RLT*. Figure 5(b) shows that the *RLT* increases with the increase in powder concentration. Increasing the powder concentration increases the material removal rate and as the machining rate increases, the *RLT* also increases provided the flushing pressure remains the same. As the T_{on} increases more amount of heat is transferred to the section at a constant flushing pressure, the dielectric fluid cannot flush the molten material and debri particles. As the T_{on} increases, the *RLT* slightly increases and then decreases tremendously with the change in concentration of powder due to the bridging effect and increase in the discharge rate thus increasing the stability of the process as shown in Fig. 5(c). With the increase in the duty cycle, the *RLT* initially increases and then subsequently decreases as shown in Fig. 5(d). This may be due to the increase in discharge duration which conducts more heat into the workpiece. With the addition of powder to the dielectric, due to the abrasion effect of the powdered particles a decrease in *RLT* is observed as the duty cycle further increases. The increase in V_g consequently increases the *RLT* as represented in Fig. 5(e). The increase in the gap voltage increases the discharge gap distance, thus reducing the effect of induced energy at the workpiece and increasing the deposition of material on the machined surface.

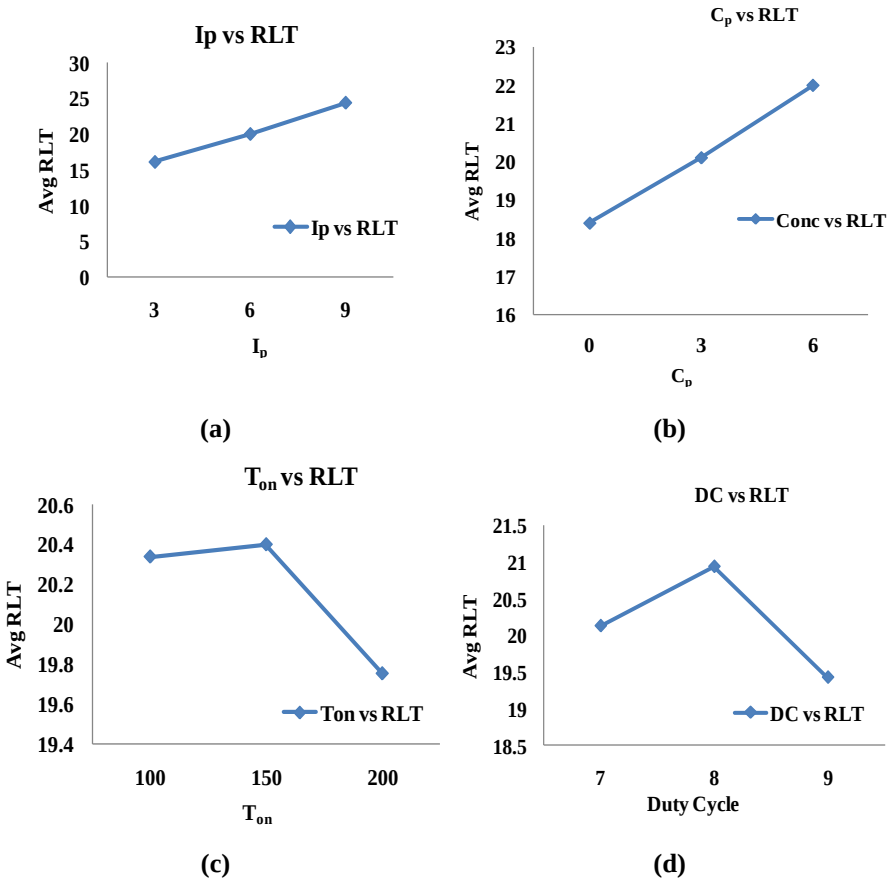

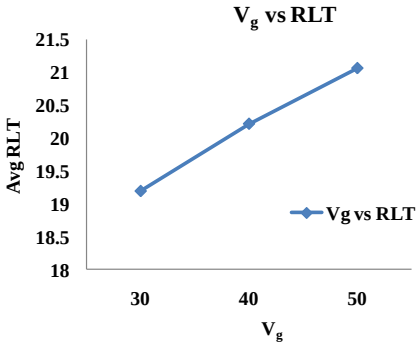

(e)

Fig. 5. Variation of RLT with the input parameters.

4.4. Effect of input parameters on micro-hardness

While examining the experimental values for *HVN* at a particular C_p, it has been observed that with the increase in I_p, the *HVN* values increase appreciably as shown in Fig. 6(a) and (b). The initial *HVN* of the parent material was almost half of the value of *HVN* obtained after machining. The *HVN* increases due to the phenomenon of melting and deposition. The experimental results reveal that as the C_p increases, the *HVN* also shows an increase with an improved surface quality. The increase in *HVN* is basically due to the re-solidification of the molten material on the machined surface. As the concentration of powder further increase, the *HVN* values also increase, which produces smoother surfaces with improved quality. It can also be observed that when the machining is carried out without the addition of powder particles, the *HVN* increases with the increase in the values of I_p and T_{on} at a particular concentration of powder as high current strengthens the pulse energy. When powdered particles are added to the dielectric, for lower values of I_p, increased *HVN* values are observed at a particular C_p which further gets increased with the increase in I_p and T_{on}. Figure 6(c) shows that with the change in T_{on}, the *HVN* values decrease as the discharge column expands with higher pulse on time. This causes more heating of the surface resulting in release of the stresses and lowering of *HVN* at higher pulse on time. Figure 6(d) shows that as the value of *DC* increases, the *HVN* decreases depending upon the pulse on time. Figure 6(e) shows the increase in *HVN* with the increase in V_g as the debri particles do not get sufficient time to get flushed away during the no spark duration.

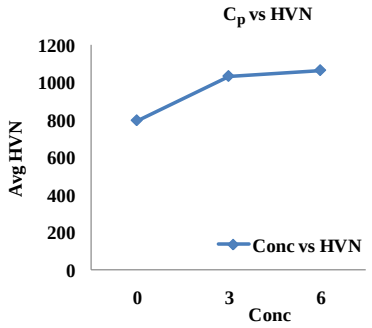

(a)

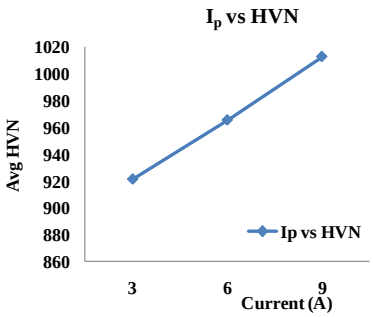

(b)

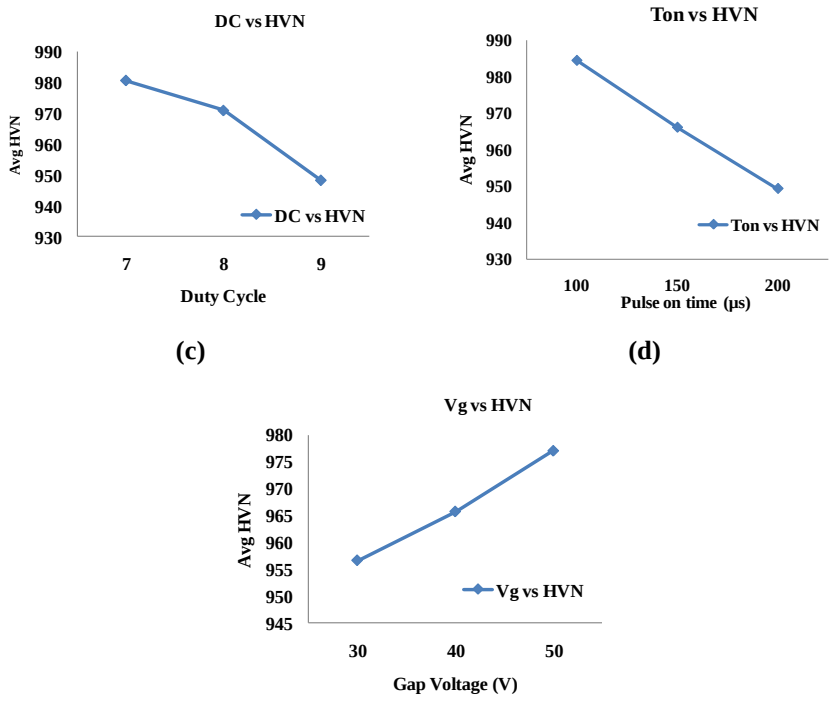

Fig. 6. Variation of HVN with the input parameters.

4.5. Grey relational analysis

The experimental results obtained for the different output parameters were first normalised using equation (3) and (4). *GRC* was calculated for each output response using equation (5). The *GRC* for each response were used to estimate the GRG using equation (6) which represents the overall performance characteristics of the machining process assuming equal weightage for all the performance characteristics considering ideal conditions. The values for *GRC* and GRG for each run with the rank order are furnished in Table 3. A multi-criteria optimization problem is thus converted to a single objective optimization problem using a combined approach of Taguchi design and GRA. Higher value of GRG leads to the optimum or close to the optimum combination of input parameters [20-22].

It can be observed that experimental run #1 is the most suitable set of performance characteristics having the highest GRG, hence it is the optimal setting followed by run #2 and #3. Separating the effect of each parameter at different levels becomes possible in case of orthogonal experimental design. Optimal parametric combination can be determined by considering the higher values of GRG. The mean GRG for each level of input parameter can be determined by estimating the averages of GRG for the particular setting of levels from the obtained experimental results. For all the levels, mean GRG can be given in the similar manner as shown in Table 4. The average of all the GRG obtained in Table 3 gives the total mean GRG. The total mean GRG is calculated to be 0.5721.

Table 3. Estimation of grey relational coefficient for performance features (ψ=0.5) and grey relational grade with rank order.

Run	GRG	Rank	Run	GRG	Rank	Run	GRG	Rank
1	0.740612	1	10	0.653818	4	19	0.626036	6
2	0.719694	2	11	0.640839	5	20	0.573795	13
3	0.676527	3	12	0.614585	7	21	0.552948	15
4	0.604177	8	13	0.536743	17	22	0.544414	16
5	0.583769	12	14	0.520255	20	23	0.523263	19
6	0.587331	11	15	0.504845	24	24	0.512719	23
7	0.588967	10	16	0.460677	27	25	0.513597	22
8	0.589243	9	17	0.474246	26	26	0.517174	21
9	0.572109	14	18	0.482712	25	27	0.531832	18

Table 4. Estimation of mean grey relational grade.

Factors	Grey Relational Grade			
	Level 1	Level 2	Level 3	Delta
C_p	0.6291	0.5430	0.5439	0.0861
I_p	0.6443	0.5463	0.5256	0.1187
T_{on}	0.5705	0.5830	0.5627	0.0466
DC	0.5845	0.5495	0.5822	0.035
V_g	0.5854	0.5713	0.5595	0.0259
Total Mean Grey Relational Grade = 0.5721				

4.5.1. Confirmatory experiment for grey relational analysis:

On identification of the optimal level of process parameters, the improvement of the performance measure is carried out by justification. The acceptable experimental results can be pragmatic by comparing the results of the confirmation tests with the predicted values. The confirmation experiments are carried out to authenticate the results drawn during the analysis and are represented in Table 5. From the optimal level of design parameters, the estimated GRG is calculated as:

$$\hat{\gamma} = \gamma_m + \sum_{i=1}^{p} \left(\bar{\gamma} - \gamma_m \right) \tag{7}$$

where γ_m is the total mean GRG, γ_i is the mean GRG at the most favourable setting and p being the number of major variables affecting the performance feature. Thus, the predicted GRG is equivalent to the mean GRG and the sum of the difference of mean GRG of each factor at the optimal level and the total mean GRG.

Figure 7 represents the S/N ratio plot for GRG with respect to all the input responses taken into consideration. The tendency of deviation of the response curves suggest that "the first level of parameters for C_p, first level of I_p, second level of T_{on}, first level of *DC* and first level of V_g" offer maximum GRG when machined using PMEDM.

Table 5. Findings from the confirmatory experiment.

Initial factor Setting		Optimal Set	
		Predicted	Experimental
Level	$C_{p2}I_{p2}T_{on2}DC_2V_{q2}$	$C_{p1}I_{p1}T_{on2}DC_1V_{q1}$	$C_{p1}I_{p1}T_{on2}DC_1V_{q1}$
Concentration of graphite powder (g/l)	3		0
Peak Current (A)	6		3
Pulse On Time (µs)	150		150
Duty Cycle (%)	8		7
Gap Voltage (V)	40		30
GRG	0.5365	0.7379	0.7390
Improvement in GRG =	0.2025		

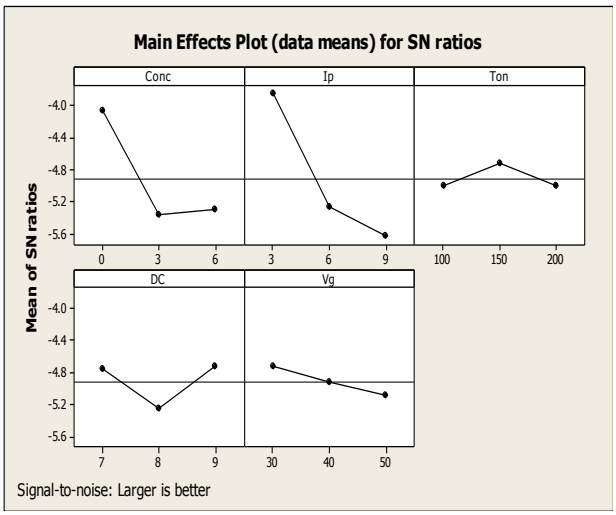

Fig. 7. S/N ratio plot for GRG.

4.5.2. ANOVA for grey relational analysis:

ANOVA, a statistical tool, is used to identify any differences in the average performance of the set of items under test. The significant effect of process variables on the response parameters can be specified using ANOVA at a 95% confidence interval. The results of factor responses have been calculated considering 'higher-the-better' expectation using MINITAB software. ANOVA result for means of GRG is given in Table 6.

The results of ANOVA exhibit that all the p-values are less than 0.05. Hence, the null hypothesis may be rejected where the independent variables do not predict the dependent variables and the alternative hypothesis may be accepted, where all the independent variables reliably predict the dependent variables. The order of percentage contributions of different input variables is $T_{on}>V_a>DC> I_p$ and C_p. The major difference between R^2 and adjusted R^2 is that R^2 assumes that every single variable explains the variation in the dependent variable where as adjusted R^2 gives the percentage of variation of the independent variables that actually affect the

dependent variable. The adjusted R^2 value was found to be 94.4%. Hence, it can be concluded that, 94.4% of the response variables fit the linear model.

Table 6. ANOVA table for GRG.

Source	DF	Seq SS	Adj SS	Adj MS	F	P
Concentration	2	9.76	9.7602	4.88	77.23	0.00
Ip	2	15.725	15.725	7.862	124.42	0.00
T_{on}	2	0.518	0.518	0.259	4.10	0.036
DC	2	1.536	1.536	0.768	12.16	0.001
V_a	2	0.586	0.586	0.293	4.64	0.026
Residual error	16	1.011	1.011	0.063		
Total	**26**	**29.138**				
S= 0.2514	**R-Sq= 96.5%**	**R-Sq(adj) = 94.4%**				

4.6. **Micro-structure analysis**

It could be seen from the micro-structure analysis that the profile of the material surface beneath the recast layer varies as shown in Figure.8. It is observed that the roughness of the surface is dependent on the recast layer distribution. The prevailing thermal conditions cause damages to the machined surface, making the surface profile uneven. The presence of the powder particles in proper concentrations and melting phenomenon plays a major role in the material modification and variation of surface properties. It is also found that foreign particles are capable of reducing the SR of the machined parts when mixed in proper quantities. The surface properties during PMEDM using graphite powder do not show much improvement in comparison to EDM due to the significant formation of carbide layer on the top surface of the machined specimen. Figure.8 shows the micro-structure of the machined specimen obtained with the optimum settings which confirm less recast layer thickness and SR. The experimental investigations show that the addition of powder particles reduces the roughness of the surface to a great extent, but the application of multi-objective optimization results in identifying the best set of parameters which optimize all the parameters simultaneously to produce a machined surface with improved properties.

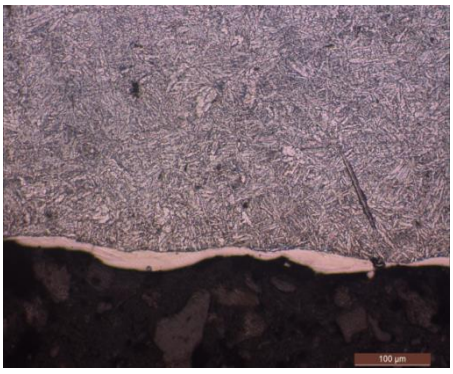

Fig. 8. Micro-structure of the workpiece at the optimal setting.

5. Conclusions

The following are the findings from the present work:

- The *MRR* shows a rise with all the significant input parameters taken into consideration as a consequence of adding required amount of powder to the dielectric.
- The *SR* reaches its maximum value during EDM and it reduces remarkably during PMEDM when the powder is added in the concentration of 3g/l. Adding powder in a concentration of 6g/l to the dielectric fluid, slightly increases the *SR*. Thus, addition of powder particles in proper concentration reduces the *SR* during machining.
- The *RLT* increases with the increase in powder concentration as the machining rate increases and the flushing pressure remains the same and the dielectric fluid cannot flush the molten material and debri particles during the pulse-off-time.
- The increase in *HVN* is due to the re-solidification of the molten material on the machined surface. During PMEDM, the *HVN* values show an increase producing smoother surfaces with improved quality. The *HVN* also tends to increase during EDM with the increase in the values of I_p and T_{on} at a particular C_p as high current strengthens the pulse energy.
- The optimal setting of process parameters is found to be C_p= 0g/l, I_p= 3A, T_{on}= 150µs, *DC* =70% and V_g = 30 V using GRA.
- Confirmatory tests reveal that the improvement of GRG in the experimental setting from the chosen set of initial parameters is 0.2025 using GRA which is satisfactory.
- While conducting the confirmatory test at the optimal set of process parameters, the surface properties exhibited increased *MRR* and *HVN* and reduced R_a, *RLT* and crack formation signifying an improvement in surface properties.
- The p-values of the input parameters (C_p=0.000, I_p=0.000, T_{on}=0.036, *DC*=0.001, V_g=0.026) are smaller in comparison to alpha value (0.05), so the null hypothesis has been rejected and the alternative hypothesis has been accepted i.e. all the independent variables reliably predict the dependent variable. Hence, all the factors show a statistically significant relationship with the dependent variables.
- ANOVA was carried out to find out the significance of machining parameters affecting process characteristics at 95 % confidence interval and the adjusted R^2 value was found to be 94.4%. Hence, it can be concluded that, 94.4% of the response variables fit the linear model.
- As demonstrated from the micro-structure analysis, the surface properties during PMEDM using graphite powder do not show much improvement in comparison to EDM due to the significant formation of carbide layer on the top surface of the machined specimen.
- Suspending powder particles to the dielectric fluid during PMEDM produces widened gap compared to EDM which facilitates the flushing action and brings stability to the process. However, the powder should be added in suitable concentrations as more powder present will settle down in the tank causing difficulty in the stirring action thus hampering the process.

- The experimental investigations show that the application of multi-objective optimization results in identifying the best set of parameters will optimize all the parameters simultaneously to produce a machined surface with improved properties.

References

1. Kobayashi, K. (1995). The present and future developments of EDM and ECM. *Proceedings of the Eleventh International Symposium for Electro Machining* (*ISEM XI), EDM Technology Transfer, Lausanne*, 29-47.
2. Pecas, P.; and Henriques, E. (2003). Influence of silicon powder mixed dielectric on conventional electrical discharge machining. *International Journal of Machine Tool and Manufacture*, 43(14), 1465-1471.
3. Ho, K.H.; and Newman, S.T. (2003). State of the art electrical discharge machining (EDM). *International Journal of Machine Tool and Manufacture*, 43(13), 1287-1300.
4. Pecas, P.; and Henriques, E. (2003). Influence of silicon powder mixed dielectric on conventional electrical discharge machining. *International Journal of Machine Tool and Manufacture*, 43, 1465-1471.
5. Pecas, P.; and Henriques, E. (2008), Electrical discharge machining using simple and powder mixed dielectric: The effect of the electrode area on the surface roughness and topography. *Journal of Materials Processing Technology*, 200(1-3), 250-258.
6. Kumar, S.; Singh, R.; Singh, T.P.; and Sethi, B.L. (2009). Surface modification by electrical discharge machining: A review. *Journal of Materials Processing Technologies*, 209(8), 3675-3687.
7. Kumar, A.; Maheswari, S.; Sharma, C.; and Beri, N. (2010). Research developments in additives mixed Electrical Discharge Machining (AEDM): A state of art review. *Materials and Manufacturing Processes*, 25(10), 1166-1180.
8. Jeswani, M.L. (1981). Effects of the addition of graphite powder to kerosene used as dielectric fluid in electrical discharge machining. *Wear*, 70(2), 133-139.
9. Kansal, H.K.; Singh, S.; and Kumar, P. (2005).Parametric optimization of powder mixed electrical discharge machining by response surface methodology. *Journal of Materials Processing Technology*, 169 (3), 427-436.
10. Kansal, H.K.; Singh, S.; and Kumar, P. (2006). Performance parameters optimization (multi-characteristics) of powder mixed electric discharge machining (PMEDM) through Taguchi's method and utility concept. *Indian Journal of Engineering and Materials Sciences*, 13(3), 209-216.
11. Singh, S.; and Yeh, M.F. (2010). Optimization of abrasive powder mixed EDM of aluminium Matrix Composites with multiple responses using gray relational analysis. *Journal of materials engineering and performance*, 21(4), 481-491.
12. Bhattacharya, A.; Batish, A.; Singh, G.; and Singla, V.K. (2012). Optimal parameter settings for rough and finish machining of die-steels in powder-mixed EDM. *International Journal of Advanced Manufacturing Technology*, 61(5), 537-548.

13. Singh, B.; Singh, P.; Tejpal, G.; and Singh, G. (2012). An experimental study of surface roughness of H-11 in EDM process using copper tool electrode. *International Journal of Advanced manufacturing Technology*, 3(4), 30-33.
14. Kansal, H.K.; Singh, S.; and Kumar, P. (2007). Effect of Silicon powder mixed EDM on machining rate of AISI D2 die steel. *Journal of Manufacturing Processes*, 9(1), 13-22.
15. Batish, A.; Bhattacharya, A.; Singla, V.K.; and Singh, G. (2012). Study of material transfer mechanism in die steels using powder mixed electrical discharge machining. *Materials and Manufacturing Processes*, 27(4), 449-456.
16. Wu, K.L.; Yan, B.H.; Huang, F.Y.; and Chen, S.C. (2005). Improvement of surface finish on SKD steel using electro-discharge machining with aluminium and surfactant added dielectric. *International Journal of Machine Tools and Manufacture*, 45(10), 1195-1201.
17. Mohri, N.; Saito, N.; and Higashi, M.A. (1991). A new process of finish machining on free surface by EDM methods. *Annals CIRP*, 40(1), 207-210.
18. Mohri, N.; Tsukamoto, J.; and Fujino, M. (1985). Mirror-like finishing by EDM. *Proceedings of the 25th International Symposium on Machine Tool Design and Research, UK*, 329-336.
19. Mohri, N.; Tsukamoto, J.; and Fujino, M. (1988). Surface modification by EDM-an innovation in EDM with semi-conductive electrodes. *Proceedings of Winter Annual meet ASME*, 34, 21-30.
20. Datta, S.; Bandyopadhyay, A.; Pal, P.K. (2008). Solving multi-criteria optimization problem in submerged arc welding consuming a mixture of fresh flux and fused slag. *International Journal of Advanced Manufacturing Technology*, 35(9), 935-942.
21. Tripathy, S.; and Tripathy, D.K. (2016). Multi-attribute optimization of machining process parameters in powder mixed electro-discharge machining using TOPSIS and grey relational analysis. *Engineering Science and Technology, an International Journal*, 19(1), 62-70.
22. Tripathy, S.; and Tripathy, D.K. (2017). Multi-response optimization of machining process parameters for powder mixed electro-discharge machining of H-11 die steel using grey relational analysis and topsis. *Machining science and technology*, 3, 362-384.